

Scaling of the higher-order flow harmonics: implications for initial-eccentricity models and the “viscous horizon”

Roy A. Lacey,^{1,*} A. Taranenko,¹ N. N. Ajitanand,¹ and J. M. Alexander¹

¹*Department of Chemistry, Stony Brook University,
Stony Brook, NY, 11794-3400, USA*

(Dated: April 26, 2019)

The ratios $v_n/(v_2)^{n/2}$ of the higher-order flow harmonics ($v_{n,n \geq 3}$) are observed to be independent of transverse momentum p_T , for a broad range of centrality selections in Au+Au and Pb+Pb collisions at $\sqrt{s_{NN}} = 0.2$ and 2.76 TeV respectively. At relatively low p_T , this scaling is compatible with the expected growth of viscous damping for sound propagation in the plasma produced in these collisions. It also provides a constraint for distinguishing between the two leading eccentricity models, as well as new estimates for the ratio of viscosity to entropy density η/s , and the “viscous horizon” or length-scale which characterizes the highest harmonic that survives viscous damping.

PACS numbers: 25.75.-q, 25.75.Dw, 25.75.Ld

Full characterization of the transport properties of the strongly interacting matter produced in heavy ion collisions, is a central goal of the experimental heavy ion programs at both the Relativistic Heavy Ion Collider (RHIC) and the Large Hadron Collider (LHC). Collective flow, as manifested by the anisotropic emission of particles in the plane transverse to the beam direction [1], continues to play an important role in these ongoing efforts [2–15]. This anisotropy can be determined, as a function of particle transverse momentum p_T and collision centrality (cent) or the number of participant nucleons N_{part} . It is characterized by Fourier coefficients v_n :

$$\frac{dN}{d\phi} \propto \left(1 + \sum_{n=1} 2v_n \cos(n\phi - n\Psi_n) \right), \quad (1)$$

and by the pair-wise distribution in the azimuthal angle difference ($\Delta\phi = \phi_a - \phi_b$) between particle pairs with transverse momenta p_T^a and p_T^b (respectively) [1, 16, 17];

$$\frac{dN^{\text{pairs}}}{d\Delta\phi} \propto \left(1 + \sum_{n=1} 2v_n^a(p_T^a)v_n^b(p_T^b) \cos(n\Delta\phi) \right), \quad (2)$$

where ϕ is the azimuthal angle of an emitted particle, and Ψ_n are the azimuths of the estimated participant event planes [18–20];

$$v_n = \langle \cos n(\phi - \Psi_n) \rangle$$

$$v_n^* = \langle \cos n(\phi - \Psi_m) \rangle, \quad n \neq m, \quad (3)$$

where the brackets denote averaging over particles and events. Here, the the starred notation is used to distinguish the n -th order moments obtained relative to the m -th order event plane Ψ_m (eg. v_4^* relative to Ψ_2). For flow driven anisotropy devoid of non flow effects, the Fourier coefficients obtained with Eqs. 1 and 2 are equivalent.

Flow coefficients result from an eccentricity-driven hydrodynamic expansion of the matter in the collision zone [6, 11–14, 21–30], *i.e.*, a finite eccentricity ε_n drives uneven pressure gradients in- and out of the event plane,

and the resulting expansion leads to the anisotropic emission of particles about this plane. The coefficients $v_n(p_T, \text{cent})$ (for odd and even n) are sensitive to both the initial eccentricity and the specific shear viscosity η/s (*i.e.* the ratio of shear viscosity η to entropy density s) of the expanding hot plasma [6–8, 10, 22, 31–35]. Here, it is noteworthy that, for symmetric systems, the symmetry transformation $\Psi_{RP} \rightarrow \Psi_{RP} + \pi$, dictates that the odd harmonics are zero for smooth eccentricity profiles. However, the “lumpy” transverse density distributions generated in actual collisions, result in eccentricity profiles which have no particular symmetry, so the odd harmonics are not required to be zero from event to event. Fortunately, the pervasive assumption of a smooth eccentricity profile has hindered full exploitation of the odd harmonics until recently [36].

Because of the acoustic nature of anisotropic flow (*i.e.* it is driven by pressure gradients), a transparent way to evaluate the strength of dissipative effects is to consider the attenuation of sound waves. In the presence of viscosity, sound intensity is exponentially damped $e^{(-r/\Gamma_s)}$ relative to the sound attenuation length Γ_s . This can be expressed in terms of a perturbation to the energy-momentum tensor $T_{\mu\nu}$ [37]:

$$\delta T_{\mu\nu}(t) = \exp\left(-\frac{2}{3}\frac{\eta}{s}\frac{k^2 t}{3T}\right) \delta T_{\mu\nu}(0), \quad (4)$$

where the spectrum of initial ($t = 0$) perturbations can be associated with the harmonics of the shape deformations and density fluctuations. Here, k is the wave number for these harmonics, and t and T are the expansion time and the temperature of the plasma respectively. The “viscous horizon” is the length scale r_v , which separates the sound wavelengths which are effectively damped out from those which are not [37], and $k_v = 2\pi/r_v$ is linked to the order (n_v) of the highest harmonic which survives viscous damping. Thus, the relative magnitudes of the higher-order harmonics ($v_{n,n \geq 3}$) are expected to provide additional constraints on both the magnitude of η/s and

the “best” model for eccentricity determinations [37–39].

The eccentricity-scaled coefficients $\frac{v_n(N_{\text{part}}, p_T)}{\varepsilon_n(N_{\text{part}})}$, plotted as a function of N_{part} , show sizable p_T -dependent deviations from the flat N_{part} dependence which are characteristic of the scale invariance of perfect fluid hydrodynamics ($\eta/s = 0$) [15]. The magnitude of the viscous corrections (and hence, η/s), has been determined via parametrization of these deviations with a Knudsen number ($K = \lambda/\bar{R}$) ansatz [8, 15, 39];

$$\frac{v_n}{\varepsilon_n} = \frac{v_n^h}{\varepsilon_n} \left[\frac{1}{1 + \frac{K(n)}{K_0}} \right] \quad n = 2, 3, \dots, \quad (5)$$

where $K(n)$ characterizes the magnitude of the viscous correction associated with the flow harmonic v_n ; v_n^h/ε_n is the eccentricity-scaled coefficient expected from ideal hydrodynamics; λ is the mean-free path; \bar{R} is the transverse size of the system ($\frac{1}{\bar{R}} = [1/\sigma_x^2 + 1/\sigma_y^2]^{1/2}$), and K_0 is a constant estimated to be 0.7 ± 0.03 with the aid of a transport model [40]. Note that $K(n)$ and η/s are both proportional to λ [15].

Since viscous damping scales as k^2 (cf. Eq. 4) the viscous corrections for the higher-order eccentricity driven harmonics (with wavelengths $2\pi\bar{R}/n$ for $n \geq 1$, *i.e.* $k \sim n/\bar{R}$), are expected to scale as $n^2 K$. Thus, their associated viscous corrections can be expressed in terms of that for the second flow harmonic, $K(n) = (n^2/4)K(2)$, suggesting a scaling relationship between $v_{n,n \geq 3}$ and v_2 . Here, we report the observation that the measured ratios $[v_n/(v_2)^{n/2}]_{n \geq 3}$ scale as a function of p_T , and show that this scaling provides: (i) important insights into viscous damping of the higher-order flow harmonics, (ii) a constraint for distinguishing between the two leading eccentricity models, *i.e.* the Glauber [41, 42] and the factorized Kharzeev-Levin-Nardi (KLN)[43, 44] models, and (iii) an independent but robust estimate of η/s .

The data for $v_n^*(p_T, \text{cent})$ and $v_n(p_T, \text{cent})$ employed in our analysis were obtained from measurements by the PHENIX collaboration, for Au+Au collisions at $\sqrt{s_{NN}} = 0.2$ TeV [20, 45], and measurements by the CMS collaboration for Pb+Pb collisions at $\sqrt{s_{NN}} = 2.76$ TeV [46]. The Au+Au data set exploits the event plane analysis method (c.f. Eq. 3), while the Pb+Pb data set utilizes the two-particle $\Delta\phi$ correlation technique (c.f. Eq. 2). Note as well that, due to partial error cancellation, the relative systematic errors for the ratios $v_n/(v_2)^{n/2}$ and $v_n^*/(v_2)^{n/2}$ are much smaller than those reported for v_n .

Figure 1 shows the ratios $v_4^*/(v_2)^2$ vs. p_T (a) and N_{part} (b) respectively for Au+Au collisions. These ratios indicate an essentially flat dependence on p_T , but show a characteristic increase with N_{part} up to $\sim 1.8 \pm 0.2$ in the 5% most central collisions [20]. This trend is in contrast to the constant value of ~ 0.5 predicted by perfect fluid hydrodynamics [47, 48], and points to the important role of the higher-order eccentricity moments and their

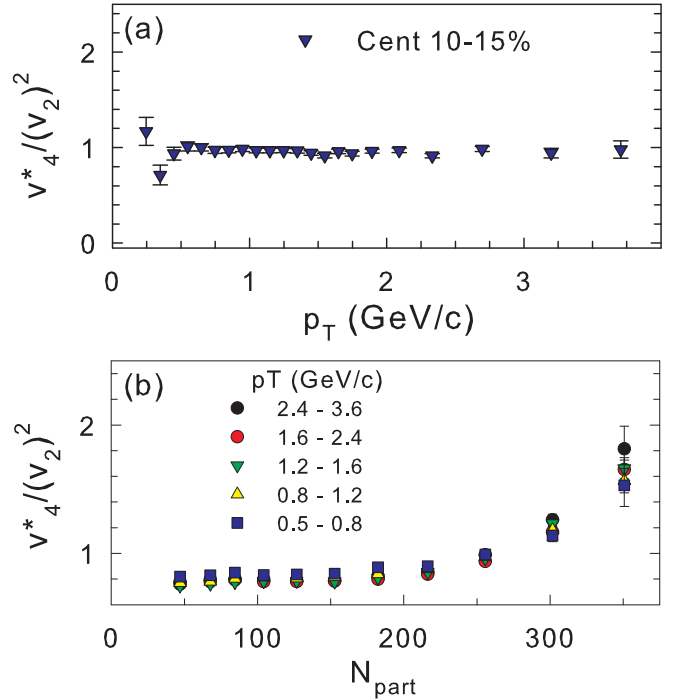


FIG. 1. (a) $v_4^*/(v_2)^2$ vs. p_T for cent = 10 – 15% and (b) $v_4^*/(v_2)^2$ vs. N_{part} for several p_T cuts, for Au+Au collisions at $\sqrt{s_{NN}} = 0.2$ TeV. The data are from Ref. [20].

fluctuations [15, 36, 38, 49, 50]. This role is made more transparent in Fig. 2, where the ratios $v_3/(v_2)^{3/2}$ and $v_4/(v_2)^2$ are plotted as a function of p_T [(a) and (b)] and N_{part} [(c) and (d)] respectively. Figs. 2 (a) and (b) show the same flat p_T dependence as in Fig. 1. However, Figs. 2 (c) and (d) indicate much larger centrality dependent magnitudes, as well as a steeper centrality dependence. The apparent differences between $v_4^*/(v_2)^2$ (Fig. 1) and $v_4/(v_2)^2$ (Fig. 2) point to the important role of ε_4 as a driver for v_4 . That is, the expected contribution to v_4 from v_2 [$\sim (v_2)^2$] does not dominate the v_4 measurements. Note as well that $v_4 > v_4^*$ is expected because the initial eccentricity fluctuations cause Ψ_4 to fluctuate about Ψ_2 .

Figure 3 compares the ratios $v_n/(v_2)^{n/2}$ (for $n = 3, 4$ and 5) in the 5% most central Pb+Pb collisions at the LHC ($\sqrt{s_{NN}} = 2.76$ TeV). Here, it is important to reiterate that these ratios have been obtained with the $v_{2,3,4,5}$ values extracted from two-particle $\Delta\phi$ correlation data [46]. We have taken these Fourier coefficients to be approximately equivalent to those determined with respect to the estimated event plane Ψ_n , *i.e.* $v_n = \langle \cos n(\phi - \Psi_n) \rangle$, because the two-particle correlation data were generated with a sizable pseudorapidity gap ($2 < \Delta\eta' < 4$) between the trigger and partner particles which comprise each pair. The ratios shown in Fig. 3 suggest a similarly flat p_T dependence (albeit with fewer data points) which appears to extend even beyond the

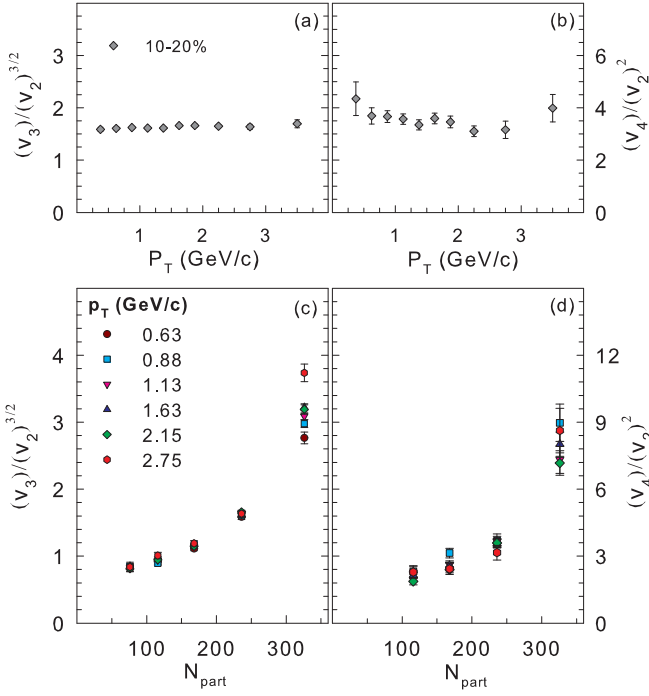


FIG. 2. (a) $v_3/(v_2)^{3/2}$ vs. p_T and (b) $v_4/(v_2)^2$ vs. p_T for Au+Au collisions. Results are shown for the 10-20% most central collisions. (c) $v_3/(v_2)^{3/2}$ vs. N_{part} and (d) $v_4/(v_2)^2$ vs. N_{part} for several p_T cuts, as indicated. The $v_{2,3,4}$ values used for these ratios are reported in Ref. [45].

151 p_T range where hydrodynamic flow is expected to break-
 152 down [15]. Note as well, that the magnitudes of these
 153 ratios are comparable to those for Au+Au collisions for
 154 the same centrality selection. We expect that future mea-
 155 surements of these ratios (in Pb+Pb collisions) for the p_T
 156 and centrality ranges shown in Figs. 1 and 2, will exhibit
 157 the same trends.

160 The scaling observed for the relatively low p_T values in
 161 Figs. 1 and 2 can be understood within the framework of
 162 Eq. 5 if $(v_n(p_T)/\varepsilon_n) = (v_2(p_T)/\varepsilon_2)^{n/2}$ [for $n \geq 3$], where

$$\left[\frac{1}{1 + \frac{K(n)}{K_0}} \right] \equiv \left[\frac{1}{1 + \frac{n^2 K(2)}{4K_0}} \right] \propto \left[\frac{1}{1 + \frac{K(2)}{K_0}} \right]^{n/2}. \quad (6)$$

163 Within errors, the latter proportionality was found to
 164 hold very well for a broad range of centralities and p_T
 165 selections, for the $K(2)$ values extracted from the eccen-
 166 tricity scaled v_2 data. Therefore, we interpret the flat
 167 p_T dependence of $v_n/(v_2)^{n/2}$ [for each cent] to be an in-
 168 dication that viscous damping for the higher harmonics
 169 follows the expected acoustic ($n^2 K$) scaling. This implies
 170 that the p_T range of validity for the parametrization in
 171 Eq. 5 should be smaller for $v_{n,n \geq 3}$ than for v_2 .

173 The proportionality indicated in Eq. 6 also sug-
 174 gests that the viscous corrections for the ratios
 175 $(v_n/\varepsilon_n)/(v_2/\varepsilon_2)^{n/2}$ essentially cancel, making them rel-
 176 atively insensitive to viscous effects. Thus, the central-

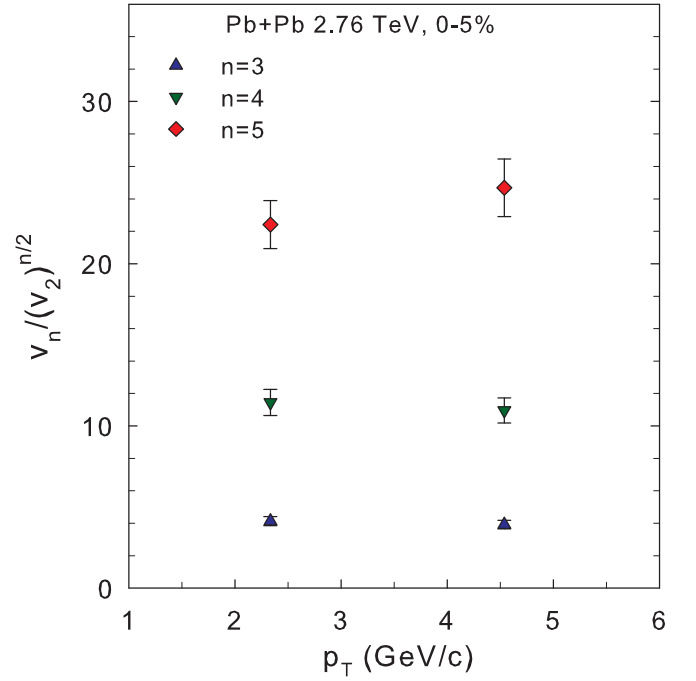


FIG. 3. $v_n/(v_2)^{n/2}$ vs. p_T for $n = 3, 4, 5$ for the 5% most central Pb+Pb collisions at $\sqrt{s_{NN}} = 2.76$ TeV. The $v_{2,3,4,5}$ values used in these ratios are extracted from the two-particle $\Delta\phi$ correlation functions reported in Ref. [46].

177 ity dependence of these ratios gives a direct constraint
 178 for the ratios $\varepsilon_n/(\varepsilon_2)^{n/2}$ and consequently, a route for
 179 distinguishing between different eccentricity models [38].
 180 The solid symbols in Fig. 4 show a representative set of
 181 the experimental $v_n/(v_2)^{n/2}$ ratios previously plotted in
 182 Figs. 2 (c) and (d). The open symbols show the corre-
 183 sponding eccentricity ratios obtained for the two eccen-
 184 tricity models. The ε_n values for these ratios were evalu-
 185 ated [via Monte Carlo (MC) calculations] from the two-
 186 dimensional profile of the density of sources in the trans-
 187 verse plane $\rho_s(\mathbf{r}_\perp)$, with weight $\omega(\mathbf{r}_\perp) = \mathbf{r}_\perp^n$ [38]. Fig.
 188 4 indicates relatively good agreement between data and
 189 the $\varepsilon_n/(\varepsilon_2)^{n/2}$ ratios, confirming the utility of $v_n/(v_2)^{n/2}$
 190 as a constraint for distinguishing between the eccentricity
 191 models [38].

192 The observed scaling of $v_n/(v_2)^{n/2}$ can also be used to
 193 estimate the magnitude of η/s and the viscous horizon,
 194 via the dependence of v_n/ε_n on n . To this end, we use
 195 Eqs. 5 and 6 in conjunction with the values of $K(2)$ and
 196 v_2^h/ε_2 extracted from the data (via fits to the plots of
 197 v_2/ε_2 vs. N_{part}), to obtain v_n/ε_n vs. N_{part} for each p_T
 198 selection. The v_n values so obtained for $N_{\text{part}} = 350$ and
 199 $p_T \sim 0.55$ GeV/c, are shown as a function of n in Fig. 4
 200 (c). They show the expected exponential decrease with n
 201 (cf. Eq. 4); a similar trend was observed for a broad se-
 202 lection of N_{part} and low p_T values. Fig. 4 (c) shows that,
 203 relative to v_2/ε_2 , the magnitude of $v_n/\varepsilon_{n,n \geq 3}$ decreases
 204 by nearly a factor of 50 for $n_v \sim 7$, i.e. v_n for $n \gtrsim 6$ or 7

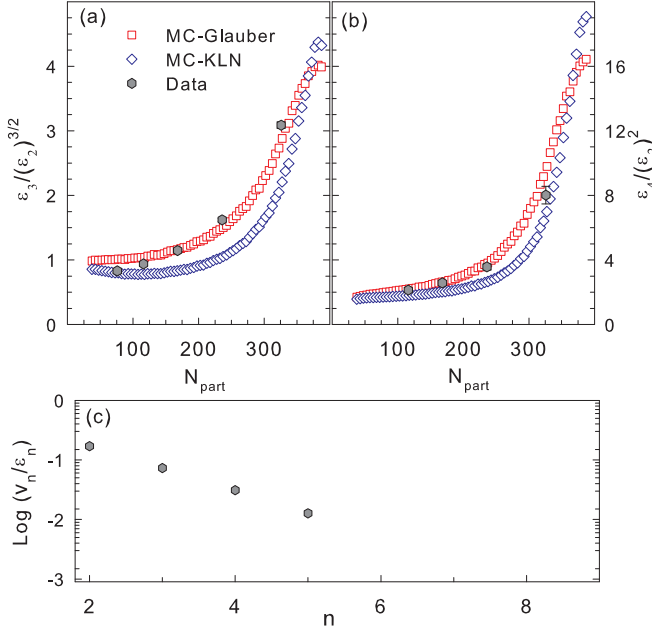


FIG. 4. Data comparisons to the calculated ratios (a) $\varepsilon_3/(\varepsilon_2)^{3/2}$ vs. N_{part} and (b) $\varepsilon_4/(\varepsilon_2)^2$ vs. N_{part} for MC-Glauber and MC-KLN initial geometries for Au+Au collisions. Calculations were performed with the weighting $\omega(\mathbf{r}_\perp) = \mathbf{r}_\perp^n$. Panel (c) shows the n dependence of v_n/ε_n (see text).

is essentially damped out. This suggests a viscous horizon $r_v = 2\pi\bar{R}/n_v \sim 1.9$ fm for central collisions.

To obtain an independent estimate of η/s , we follow Eq. 4 and perform exponential fits ($ae^{-x/b}$) to the plots of v_n/ε_n vs. n , for several p_T selections at a given value of N_{part} . For each N_{part} , the value for η/s was then obtained from the fit parameter b , following an extrapolation to $p_T = 0$. Note that this approach provides a much tighter constraint for η/s , because it is the relative values of v_n/ε_n which now effect the constraint. This procedure gives an estimate $4\pi\eta/s \sim 1.4 \pm 0.2$ in central collisions for $T = 220 \pm 20$ MeV [51] and $t = 9$ fm [52] which is in good agreement with the values from prior extractions [4–8, 10, 11, 14, 49, 53]. A similar estimate of η/s is obtained for LHC data ($\sqrt{s_{NN}} = 2.76$ TeV) [54] when the values of $v_2/\varepsilon_2(\text{cent}, p_T)$ are taken in concert with the scaling implied in Fig. 3. Here, the larger freeze out time [55] is compensated for, by a higher estimated mean temperature.

In summary, we have observed that the ratios $v_n/(v_2)^{n/2}$ of the higher-order flow harmonics ($v_{n,n \geq 3}$) are essentially independent of p_T for a broad range of centrality selections in Au+Au and Pb+Pb collisions at $\sqrt{s_{NN}} = 0.2$ and 2.76 TeV respectively. Within a parametrized viscous hydrodynamical framework, this scaling can be understood to be a consequence of the acoustic nature of anisotropic flow, *i.e.*, the observed viscous damping is characteristic of sound propagation in

the plasma produced in these collisions. This interpretation not only provides a straightforward constraint for distinguishing between the two leading eccentricity models, it gives the independent estimate $4\pi\eta/s = 1.4 \pm 0.2$ for the averaged specific shear viscosity, and $r_v \sim 1.9$ fm for the viscous horizon. The observed scaling also has important implications for accurate decomposition of flow and jet contributions to two-particle $\Delta\phi$ correlation functions. This is because the higher-order harmonics can be expressed as a power of the high precision v_2 harmonic. It will be valuable to perform further detailed studies of $v_n/(v_2)^{n/2}$ for both identified and unidentified hadrons, and to establish the p_T value which signals a breakdown of the observed scaling.

Acknowledgments This research is supported by the US DOE under contract DE-FG02-87ER40331.A008.

-
- * E-mail: Roy.Lacey@Stonybrook.edu
- [1] R. A. Lacey, Nucl. Phys. **A698**, 559 (2002); R. J. M. Snellings, *ibid.* **A698**, 193 (2002).
 - [2] M. Gyulassy and L. McLerran, Nucl. Phys. **A750**, 30 (2005).
 - [3] D. Molnar and P. Huovinen, Phys. Rev. Lett. **94**, 012302 (2005), arXiv:nucl-th/0404065.
 - [4] R. A. Lacey *et al.*, Phys. Rev. Lett. **98**, 092301 (2007).
 - [5] A. Adare *et al.*, Phys. Rev. Lett. **98**, 172301 (2007).
 - [6] P. Romatschke and U. Romatschke, Phys. Rev. Lett. **99**, 172301 (2007).
 - [7] Z. Xu, C. Greiner, and H. Stoecker, Phys. Rev. Lett. **101**, 082302 (2008).
 - [8] H.-J. Drescher, A. Dumitru, C. Gombeaud, and J.-Y. Ollitrault, Phys. Rev. **C76**, 024905 (2007).
 - [9] E. Shuryak, Prog. Part. Nucl. Phys. **62**, 48 (2009).
 - [10] M. Luzum and P. Romatschke, Phys. Rev. **C78**, 034915 (2008).
 - [11] H. Song and U. W. Heinz, J. Phys. **G36**, 064033 (2009).
 - [12] K. Dusling and D. Teaney, Phys. Rev. **C77**, 034905 (2008), arXiv:0710.5932 [nucl-th].
 - [13] P. Bozek and I. Wyskiel, PoS **EPS-HEP-2009**, 039 (2009), arXiv:0909.2354 [nucl-th].
 - [14] G. S. Denicol, T. Kodama, and T. Koide, (2010), arXiv:1002.2394 [nucl-th].
 - [15] R. A. Lacey *et al.*, (2010), arXiv:1005.4979 [nucl-ex].
 - [16] K. Adcox *et al.*, Phys. Rev. Lett. **89**, 212301 (2002).
 - [17] A. Mocsy and P. Sorensen, (2010), arXiv:1008.3381 [hep-ph].
 - [18] J.-Y. Ollitrault, Phys. Rev. **D46**, 229 (1992).
 - [19] A. M. Poskanzer and S. A. Voloshin, Phys. Rev. **C58**, 1671 (1998).
 - [20] and A. Adare (The PHENIX), (2010), arXiv:1003.5586 [nucl-ex].
 - [21] U. Heinz and P. Kolb, Nucl. Phys. **A702**, 269 (2002).
 - [22] D. Teaney, Phys. Rev. **C68**, 034913 (2003).
 - [23] P. Huovinen, P. F. Kolb, U. W. Heinz, P. V. Ruuskanen, and S. A. Voloshin, Phys. Lett. **B503**, 58 (2001).
 - [24] T. Hirano and K. Tsuda,

- Phys. Rev. **C66**, 054905 (2002), arXiv:nucl-th/0205043.
- [25] R. Andrade *et al.*, Eur. Phys. J. **A29**, 23 (2006), arXiv:nucl-th/0511021.
- [26] C. Nonaka, N. Sasaki, S. Muroya, and O. Miyamura, Nucl. Phys. **A661**, 353 (1999), arXiv:nucl-th/9907046.
- [27] H. Niemi, K. J. Eskola, and P. V. Ruuskanen, Phys. Rev. **C79**, 024903 (2009), arXiv:0806.1116 [hep-ph].
- [28] R. Peschanski and E. N. Sardiak, Phys. Rev. **C80**, 024907 (2009), arXiv:0906.0941 [nucl-th].
- [29] H. Holopainen, H. Niemi, and K. J. Eskola, (2010), arXiv:1007.0368 [hep-ph].
- [30] B. Schenke, S. Jeon, and C. Gale, (2010), arXiv:1009.3244 [hep-ph].
- [31] U. W. Heinz and S. M. H. Wong, Phys. Rev. **C66**, 014907 (2002).
- [32] R. A. Lacey and A. Taranenko, PoS **CFRNC2006**, 021 (2006).
- [33] H. Song and U. W. Heinz, Phys. Rev. **C77**, 064901 (2008).
- [34] V. Greco, M. Colonna, M. Di Toro, and G. Ferini, (2008), arXiv:0811.3170 [hep-ph].
- [35] A. K. Chaudhuri, (2009), arXiv:0910.0979 [nucl-th].
- [36] B. Alver and G. Roland, Phys. Rev. **C81**, 054905 (2010), arXiv:1003.0194 [nucl-th].
- [37] P. Staig and E. Shuryak, (2010), arXiv:1008.3139 [nucl-th].
- [38] R. A. Lacey, R. Wei, N. N. Ajitanand, and A. Taranenko, (2010), arXiv:1009.5230 [nucl-ex].
- [39] B. H. Alver, C. Gombeaud, M. Luzum, and J.-Y. Ollitrault, (2010), arXiv:1007.5469 [nucl-th].
- [40] C. Gombeaud and J. Y. Ollitrault, Phys. Rev. **C77**, 054904, 2008.
- [41] B. Alver *et al.*, Phys. Rev. Lett. **98**, 242302 (2007).
- [42] M. L. Miller, K. Reygers, S. J. Sanders, and P. Steinberg, Ann. Rev. Nucl. Part. Sci. **57**, 205 (2007).
- [43] T. Lappi and R. Venugopalan, Phys. Rev. **C74**, 054905 (2006).
- [44] H.-J. Drescher and Y. Nara, Phys. Rev. **C76**, 041903 (2007).
- [45] S. Esumi, in: Proc. of the Winter Workshop on nuclear Dynamics, 2011.
- [46] Christof Roland, Talk given at the LHC Physics Center at CERN, March 4th, 2011.
- [47] N. Borghini and J.-Y. Ollitrault, Phys. Lett. **B642**, 227 (2006).
- [48] M. Csanad, T. Csorgo, and B. Lorstad, Nucl. Phys. **A742**, 80 (2004), arXiv:nucl-th/0310040.
- [49] R. A. Lacey, A. Taranenko, and R. Wei, (2009), arXiv:0905.4368 [nucl-ex].
- [50] R. A. Lacey *et al.*, Phys. Rev. **C81**, 061901 (2010), arXiv:1002.0649 [nucl-ex].
- [51] A. Adare *et al.* (PHENIX), (2008), arXiv:0804.4168 [nucl-ex].
- [52] S. Afanasiev *et al.* (PHENIX), Phys. Rev. Lett. **100**, 232301 (2008), arXiv:0712.4372 [nucl-ex].
- [53] K. Dusling, G. D. Moore, and D. Teaney, (2009), arXiv:0909.0754 [nucl-th].
- [54] K. Aamodt *et al.* (The ALICE), (2010), arXiv:1011.3914 [nucl-ex].
- [55] K. Aamodt *et al.* (ALICE), Phys. Lett. **B696**, 328 (2011), arXiv:1012.4035 [nucl-ex].